

## DNA-Templated Ag Nanocluster Formation

Jeffrey T. Petty,<sup>\*,†</sup> Jie Zheng, Nicholas V. Hud, and Robert M. Dickson<sup>\*</sup>*Contribution from the School of Chemistry and Biochemistry, Georgia Institute of Technology, Atlanta, Georgia 30332-0400*

Received December 23, 2003; E-mail: dickson@chemistry.gatech.edu; jeff.petty@furman.edu

**Abstract:** The high affinity of Ag<sup>+</sup> for DNA bases has enabled creation of short oligonucleotide-encapsulated Ag nanoclusters without formation of large nanoparticles. Time-dependent formation of cluster sizes ranging from Ag<sub>1</sub> to Ag<sub>n</sub>/oligonucleotide were observed with strong, characteristic electronic transitions between 400 and 600 nm. The slow nanocluster formation kinetics enables observation of specific aqueous nanocluster absorptions that evolve over a period of 12 h. Induced circular dichroism bands confirm that the nanoclusters are associated with the chiral ss-DNA template. Fluorescence, absorption, mass, and NMR spectra all indicate that multiple species are present, but that their creation is both nucleotide- and time-dependent.

## Introduction

As bulk metals are devoid of a band gap, metal nanoclusters must be extremely small to exhibit discrete electronic transitions and strong fluorescence. The change in optical, magnetic, electronic, and catalytic properties with size have therefore motivated many studies of metal nanoparticles.<sup>1–3</sup> These small particles with 1–100-nm diameters are produced via the reduction of metal cations, and their rate of growth is controlled using ligands that coordinate with the metal atoms.<sup>4</sup> Surfactants, thiols, amines, carboxylic acids, and even dendrimers are all quite useful to bind, stabilize, concentrate, and direct growth of metal nanoparticles. Recently, poly(amidoamine) dendrimers (PAMAM) have been shown to stabilize even smaller Ag and Au nanoclusters with well-defined sizes while the surrounding polymeric matrix protects the developing nanoclusters against agglomeration following reduction.<sup>3</sup> Biological macromolecules have also served as templates for nanoparticle synthesis. For example, the amine functional groups of peptides assemble silver and gold cations and then cap the growing nanoparticle surface following reduction of the cations.<sup>5</sup> Another biological system of significant interest has been DNA because its large aspect ratio (length:diameter) allows the possibility of forming wires for use in nanoelectronics.<sup>6</sup> DNA has a high affinity for metal cations, and these localized cations can be reduced to form

metallic nanoparticles that follow the contour of the DNA template.<sup>6–8</sup>

One reason for controlling the size of metal nanoparticles is to understand and utilize the strong size dependence of their electronic and optical properties.<sup>1</sup> We are particularly interested in the strong, size-dependent optical properties of small (2–8 atoms) Ag nanoclusters. Along the atom to bulk transition, discrete atomic energy levels merge into highly polarizable, continuous, plasmon-supporting bands. When sufficiently small, silver nanoclusters exhibit very strong absorption and emission, making them nearly ideal fluorophores for single molecule spectroscopy. Photochemically generated nanoclusters have strong fluorescence, and they can be optically interrogated, suggesting potential utility in high-density optical data storage<sup>9</sup> and as biological labels.<sup>10</sup> In this work, we utilize specific DNA–Ag interactions to further concentrate and narrow the Ag nanocluster distributions in aqueous solutions. The fine control of nanocluster size possible in DNA, its sequence specificity, and its potential to pattern materials on surfaces suggest many further uses ranging from biology to nanoscience.

## Experimental Section

Silver nitrate (Aldrich, 99.998%) and sodium borohydride (Fisher, 98%) were used as received. Oligonucleotides (Integrated DNA Technologies) were purified by desalting by the manufacturer. The 12-base oligonucleotide 5'-AGGTCGCCGCC-3' was received as dehydrated pellets and dissolved in a 5 mM phosphate buffer (pH = 7.5). This oligonucleotide sequence was used as it favors the single-stranded vs hairpin or self-dimer forms. Concentrations were based on the

<sup>†</sup> Permanent address: Department of Chemistry, Furman University, Greenville, SC 29613.

- (1) Link, S.; El-Sayed, M. A. *J. Phys. Chem. B* **1999**, *103*, 8410–8426.
- (2) (a) Shipway, A. N.; Willner, I. *Chem. Commun.* **2001**, 20 2035–2045. (b) Petit, C.; Taleb, A.; Pileni, M. P. *Adv. Mater.* **1998**, *10*, 259–261.
- (3) Crooks, R. M.; Lemon, B. I.; Sun, L.; Yeung, L. K.; Zhao, M. Q. Dendrimer-Encapsulated Metals and Semiconductors: Synthesis, Characterization, and Applications. In *Dendrimers III: Design, Dimension, Function*; Vögtle, F., Ed.; Springer Verlag: Berlin, 2001; Vol. 212, pp 81–135.
- (4) Murray, C. B.; Kagan, C. R.; Bawendi, M. G. *Annu. Rev. Mater. Sci.* **2000**, *30*, 545–610.
- (5) Slocik, J. M.; Moore, J. T.; Wright, D. W. *Nano Lett.* **2002**, *2*, 169–173.
- (6) (a) Braun, E.; Eichen, Y.; Sivan, U.; Ben-Yoseph, G. *Nature* **1998**, *391*, 775–778. (b) Niemeyer, C. M. *Angew. Chem., Int. Ed.* **2001**, *40*, 4128–4158.

- (7) (a) Richter, J.; Seidel, R.; Kirsch, R.; Mertig, M.; Pompe, W.; Plaschke, J.; Schackert, H. K. *Adv. Mater.* **2000**, *12*, 507–510. (b) Richter, J.; Mertig, M.; Pompe, W.; Monch, I.; Schackert, H. K. *Appl. Phys. Lett.* **2001**, *78*, 536–538. (c) Mertig, M.; Ciacchi, L. C.; Seidel, R.; Pompe, W.; De Vita, A. *Nano Lett.* **2002**, *2*, 841–844.
- (8) Monson, C. F.; Woolley, A. T. *Nano Lett.* **2003**, *3*, 359–363.
- (9) (a) Peyser, L. A.; Vinson, A. E.; Bartko, A. P.; Dickson, R. M. *Science* **2001**, *291*, 103–106. (b) Peyser, L. A.; Lee, T. H.; Dickson, R. M. *J. Phys. Chem. B* **2002**, *106*, 7725–7728.
- (10) Zheng, J.; Dickson, R. M. *J. Am. Chem. Soc.* **2002**, *124*, 13982–13983.

nearest-neighbor approximations for the molar absorptivities. Reactions were conducted in either 5 mM phosphate or 100 mM NaClO<sub>4</sub>/5 mM phosphate buffer.<sup>11</sup> The silver nanoclusters were synthesized by first cooling the solution of DNA and Ag<sup>+</sup> to 0 °C and then adding NaBH<sub>4</sub> followed by vigorous shaking.

Visible absorption spectra were acquired using a Shimadzu UV-2101PC spectrometer. Circular dichroism spectra were obtained from a Jasco J-710 spectropolarimeter. Fluorescence spectra were acquired on a Shimadzu RF-5301PC spectrofluorimeter. Mass spectra were acquired using a Micromass Quattro LC operated in negative ion mode with 2.5 kV needle and 40 V cone voltages. NMR spectra were acquired on a Bruker DRX 500 operating at 500 MHz.

## Results and Discussion

**Base Association.** Ag<sup>+</sup> strongly favors association with the heterocyclic bases and not the phosphates.<sup>12,13</sup> Supporting evidence comes from spectroscopic shifts for the Ag<sup>+</sup>-laden DNA complexes, the insensitivity of the affinity to competing cations, and the higher affinity for single-stranded vs double-stranded DNA.<sup>14,15</sup> Thermodynamic measurements indicate at least two modes of binding.<sup>15,16</sup> For Ag<sup>+</sup>:base concentrations <0.2, complexes form with the purines via nitrogen or  $\pi$ -electron coordination. For higher silver concentrations (0.2 < Ag<sup>+</sup>:base < 0.5), a weaker complex forms and involves coordination with the nitrogens of either the purines or pyrimidines. In our studies, we also find changes in the electronic absorption and circular dichroism spectra that indicate the silver ions and nanoclusters associate with the bases. For the 12-base oligonucleotide, the DNA absorption maximum ( $\lambda_{\max}$ ) shifts from 257 to 267 nm upon Ag<sup>+</sup> complexation (1 Ag<sup>+</sup>:2 bases) (Figure 1). Following reduction of the bound ions, further spectral changes occur. Initially,  $\lambda_{\max}$  shifts from 267 to 256 nm, and the molar absorptivity increases. This latter effect may be attributed to new, overlapping electronic bands for small silver clusters, which are known to absorb in this spectral region.<sup>17</sup> Alternatively, the dipole coupling between the excited electronic states of the bases could be altered by structural changes induced by the silver nanoclusters, a possibility also suggested by the circular dichroism spectra (vide infra). Eventually, as Ag nanoclusters grow and visible absorptions evolve (vide infra), the  $\lambda_{\max}$  shifts to 262 nm and the molar absorptivity decreases.

The electronic transition of the bases exhibit a small circular dichroism (CD) due to the chirality of the riboses, and this spectroscopic technique is sensitive to the arrangement of the bases.<sup>18</sup> For the Ag<sup>+</sup> complex with double-stranded DNA, circular and linear dichroism studies show that Ag<sup>+</sup> induces nonplanar and tilted orientations of the bases relative to the helical axis.<sup>11</sup> For the single-stranded oligonucleotide, we observed CD spectra that are similar to those for double-stranded DNA, suggesting that Ag<sup>+</sup> may cause similar perturbation of

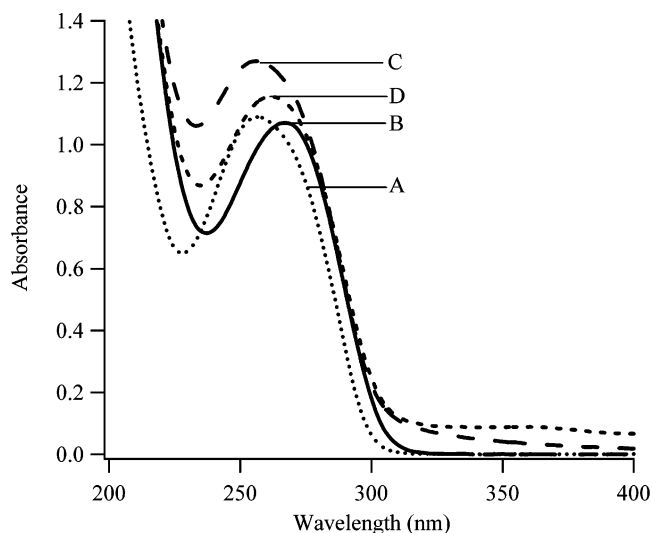


**Figure 1.** Response of the electronic transition of the oligonucleotide bases to association with Ag<sup>+</sup> and Ag nanoclusters. Following are the conditions for the spectra: A (dotted line), 10  $\mu$ M oligonucleotide solution; B (solid line), oligonucleotide with 60  $\mu$ M Ag<sup>+</sup> (1 Ag<sup>+</sup>:2 bases); C (coarse dashed line), 2 min after adding 1 BH<sub>4</sub><sup>-</sup>:1 Ag<sup>+</sup> to the oligonucleotide/Ag<sup>+</sup> solution; D (fine dashed line), 1100 min after adding BH<sub>4</sub><sup>-</sup> to the oligonucleotide/Ag<sup>+</sup> solution.

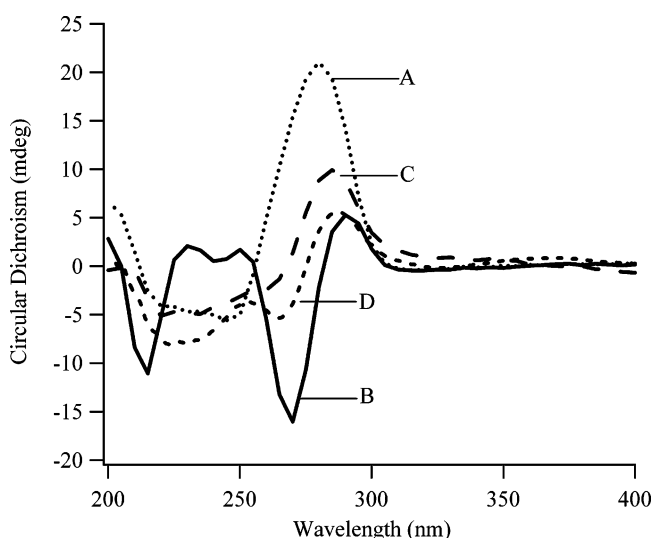


**Figure 2.** Response of the circular dichroism associated with electronic transition of the oligonucleotide bases to association with Ag<sup>+</sup> and Ag nanoclusters. Following are the conditions for the spectra: A (dotted line), 10  $\mu$ M oligonucleotide solution; B (solid line), oligonucleotide with 60  $\mu$ M Ag<sup>+</sup> (1 Ag<sup>+</sup>:2 bases); C (coarse dashed line), 120 min after adding 1 BH<sub>4</sub><sup>-</sup>:1 Ag<sup>+</sup> to the oligonucleotide/Ag<sup>+</sup> solution; D (fine dashed line), 4300 min after adding BH<sub>4</sub><sup>-</sup> to the oligonucleotide/Ag<sup>+</sup> solution.

the bases in single-stranded DNA (Figure 2). Analogous to the evolution of the absorption spectra (Figure 1), the CD spectra also change upon reduction of the Ag<sup>+</sup>. The differences between the spectra in Figure 2 indicate that the silver nanoclusters induce different structural changes in DNA than does Ag<sup>+</sup>.

**Nanocluster Sizes.** Because of the monodispersity of synthesized DNA oligonucleotides, the stoichiometry of the nanoclusters can be accurately determined using electrospray mass spectrometry (Figure 3). These experiments were conducted in water to reduce the concentrations of cations that would form adducts with the DNA and consequently reduce sensitivity. The experiments also used a higher concentration of oligonucleotide (75  $\mu$ M) to enhance the ion abundance. In Figure 3A, the

- (11) Norden, B.; Matsuoka, Y.; Kurucsev, T. *Biopolymers* **1986**, *25*, 1531–1545.
- (12) Eichhorn, G. L. Complexes of Nucleosides and Nucleotides. In *Inorganic Biochemistry*; Eichhorn, G. L., Ed.; Elsevier: New York, 1973; Vol. 2, Chapter 33.
- (13) Marzilli, L. G. Metal-Ion Interactions with Nucleic Acids and Nucleic Acid Derivatives. In *Progress in Inorganic Chemistry*; Lippard, S. J., Ed.; John Wiley and Sons: New York, 1977; Vol. 23, pp 255–378.
- (14) Luk, K. F. S.; Maki, A. H.; Hoover, R. J. *J. Am. Chem. Soc.* **1975**, *97*, 1241–1242.
- (15) Yamane, T.; Davidson, N. *Biochim. Biophys. Acta* **1962**, *55*, 609–621.
- (16) Dattagupta, N.; Crothers, D. M. *Nucleic Acids Res.* **1981**, *9*, 2971–2985.
- (17) Harbich, W.; Fedrigo, S.; Meyer, F.; Lindsay, D. M.; Lignieres, J.; Rivoal, J. C.; Kreisler, D. *J. Chem. Phys.* **1990**, *93*, 8535–8543.
- (18) Rodger, A.; Norden, B. *Circular Dichroism and Linear Dichroism*; Oxford: New York, 1997.

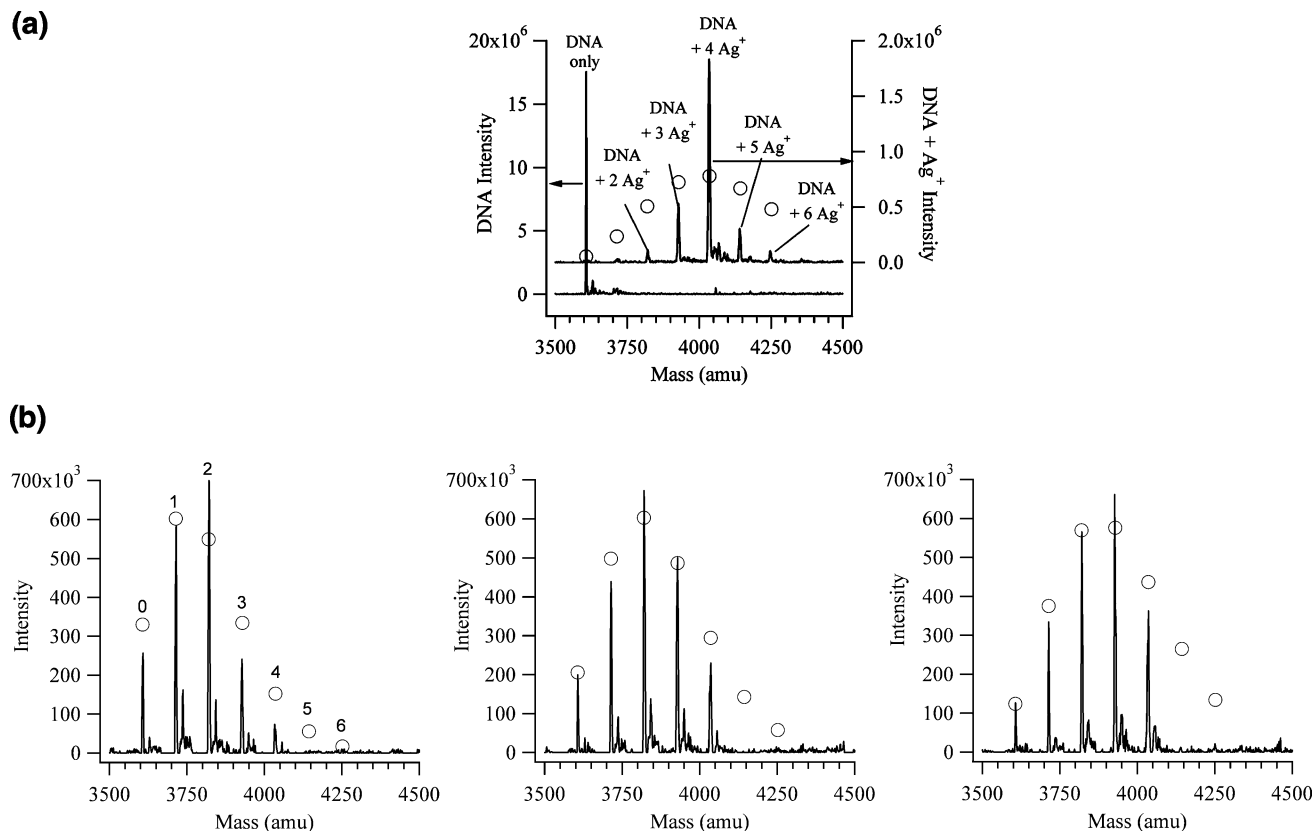


**Figure 3.** (a) Electrospray ionization mass spectra of the oligonucleotide and silver ion adducts. Following are the conditions for the spectra: Left axis: 75  $\mu\text{M}$  oligonucleotide solution with a peak at 3607 amu. Right axis: 75  $\mu\text{M}$  oligonucleotide with 450  $\mu\text{M}$   $\text{Ag}^+$  (1  $\text{Ag}^+$ :2 bases) with peaks at 3821, 3928, 4035, 4141, and 4247 amu. The intensities of the peaks for the  $\text{Ag}^+$ /DNA complexes were fit with a Poisson distribution (O) to give a mean size of  $4.3 \pm 1.3$   $\text{Ag}^+$ /oligonucleotide. (b) Electrospray ionization mass spectra of silver cluster complexes with the DNA oligonucleotide. Overlaid as open circles are the Poisson fits of the intensity distributions. Following are the conditions for the spectra with the mean number of bound Ag provided in parentheses: Left: 75  $\mu\text{M}$  oligonucleotide with 60  $\mu\text{M}$   $\text{Ag}^+$  and 50 min after adding 1  $\text{BH}_4^-$ :1  $\text{Ag}^+$  ( $1.8 \pm 0.3$  Ag). Middle: 350 min after adding  $\text{BH}_4^-$  to the oligonucleotide/ $\text{Ag}^+$  solution ( $2.4 \pm 0.2$  Ag). Right: 1050 min after adding  $\text{BH}_4^-$  to the oligonucleotide/ $\text{Ag}^+$  solution ( $3.0 \pm 0.2$  Ag). The peaks are observed at 3607, 3714, 3821, 3927, and 4036 amu. The small peaks displaced by 23 amu are attributed to Na–DNA adducts due to the use of  $\text{NaBH}_4$  for the reduction.

dominant peak in the spectrum occurs at 3607 amu, as expected for the 12-base oligonucleotide. Addition of 6  $\text{Ag}^+$ :oligonucleotide (1  $\text{Ag}^+$ :2 bases) results in complexes with a maximum of 4  $\text{Ag}^+$  per DNA strand. This difference between the total and bound ion concentrations may be attributed to the weaker adducts that form at higher silver concentrations,<sup>15</sup> which may be more susceptible to dissociation during desolvation and/or ionization. A poor description of the ion intensities is observed when they are fit as a Poisson distribution, which suggests that 4  $\text{Ag}^+$ /oligonucleotide is the favored stoichiometry (Figure 3a). The DNA sequence used for these studies favors the single-stranded form as opposed to self-duplex or hairpin forms. The mass spectra indicate that the clusters are also bound to a single DNA strand. Following reduction of the bound  $\text{Ag}^+$  ions, the number of bound silver atoms is initially small, but the distribution shifts to higher stoichiometries with time (Figure 3b). As opposed to the  $\text{Ag}^+$  complexes, a Poisson distribution gives a more accurate description of the ion distributions for the reduced complexes. The following average cluster sizes were measured:  $1.8 \pm 0.3$  (50 min),  $2.4 \pm 0.2$  (350 min), and  $3.0 \pm 0.2$  (1050 min). The observed distribution terminates at 4  $\text{Ag}$ /oligonucleotide, which again differs from a Poisson distribution. End effects may contribute to the stoichiometries of both the ion and metal complexes with these short oligonucleotides, but spectroscopic studies directly suggest that the base sequence is a significant feature of the interaction of the nanoclusters with

DNA (vide infra). The mass spectra do not distinguish the possibility of single clusters or multiple smaller clusters bound to a single oligonucleotide, and studies with oligonucleotides of varying lengths and sequences may resolve this issue.

**Nanocluster Spectra.** Mass spectrometry demonstrates that a small number ( $\leq 4$ ) of silver atoms are bound to the single-stranded DNA template, and the following spectroscopic studies demonstrate that these silver atoms form nanoclusters. Reduction of the  $\text{Ag}^+$  bound to the DNA results in new species with electronic transitions in the visible region of the spectrum (Figure 4). The transition that is most prominent initially has a  $\lambda_{\text{max}} = 426$  nm at 9 min after adding the  $\text{BH}_4^-$ . Over a period of 12 h, the absorbance of this band decreases and a broad absorption band with peaks at 424 and 520 nm develops. As determined through theoretical and low-temperature spectroscopic studies, electronic transitions for small silver clusters, in particular  $\text{Ag}_2$  and  $\text{Ag}_3$ , are expected in this spectral region.<sup>17,19,20</sup> A definitive assignment of the electronic bands is problematic using these prior studies because the peaks for the DNA-bound cluster are expected to shift and broaden relative to their gas phase and rare gas matrix-isolated values. No change in the absorbances or peak positions is observed when the

(19) Bonacic-Koutecky, V.; Pittner, J.; Boiron, M.; Fantucci, P. *J. Chem. Phys.* **1999**, *110*, 3876–3886.

(20) Marchetti, A. P.; Muentner, A. A.; Baetzold, R. C.; McCleary, R. T. *J. Phys. Chem. B* **1998**, *102*, 5287–5297.

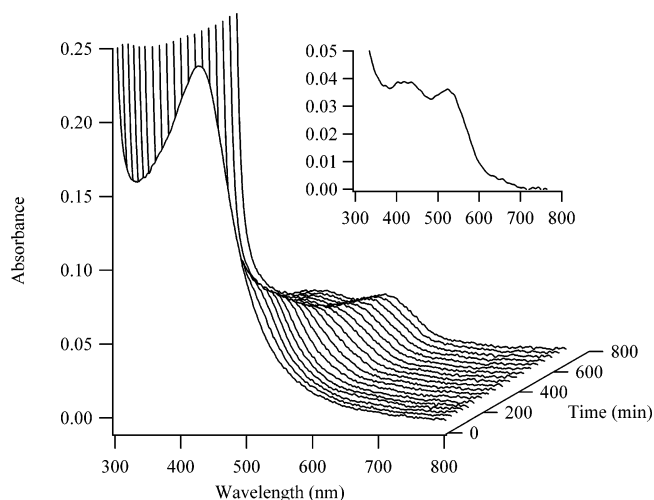


**Figure 4.** Absorption spectra associated with the DNA-bound silver nanoclusters. For these spectra, [oligonucleotide] = 10  $\mu\text{M}$ ,  $[\text{Ag}^+] = 60 \mu\text{M}$ , and  $[\text{BH}_4^-] = 60 \mu\text{M}$ . The foremost spectrum in the time series was acquired 9 min after adding the  $\text{BH}_4^-$ , and it has  $\lambda_{\text{max}} = 426 \text{ nm}$ . Subsequent spectra were acquired approximately every 30 min. The inset spectrum shows the last spectrum in the series (692 min), and peaks are observed at 424 and 520 nm.

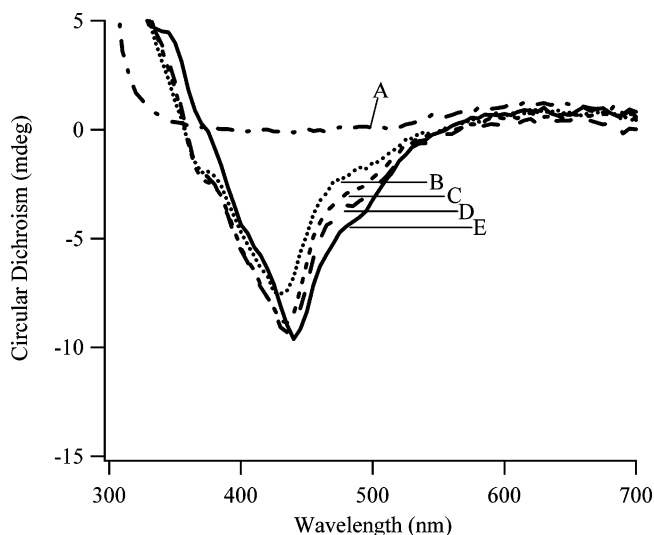


**Figure 5.** Induced circular dichroism spectra for the electronic transitions associated with the nanoclusters. For these spectra, [oligonucleotide] = 10  $\mu\text{M}$ ,  $[\text{Ag}^+] = 60 \mu\text{M}$ , and  $[\text{BH}_4^-] = 60 \mu\text{M}$ , and the cell path length was 5 cm. The spectra were collected 2 min (A, dashed-dotted line), 20 min (B, dotted line), 40 min (C, fine dashed line), 60 min (D, coarse dotted line), and 150 min (E, solid line) after adding the  $\text{BH}_4^-$ .

solutions are centrifuged, indicating that the spectra cannot be attributed to nanoparticles. Similar spectra are observed when 2  $\text{BH}_4^-:1 \text{ Ag}^+$  is used, indicating that the spectra arise from fully reduced silver clusters (not shown). In a buffer with 100 mM  $\text{NaClO}_4$ , the results are similar to those in the lower salt buffer, with the only difference being a broad band without distinct peaks after longer times. This similarity suggests nanocluster formation is not impeded by competing cations, which is consistent with their association via the bases and not the phosphates.

Because the small silver clusters do not have inherent chirality, the induced CD associated with the Ag nanocluster electronic transitions is further evidence that the clusters are bound to the DNA (Figure 5). The most prominent band has a minimum response at 440 nm, and this minimum shifts to longer

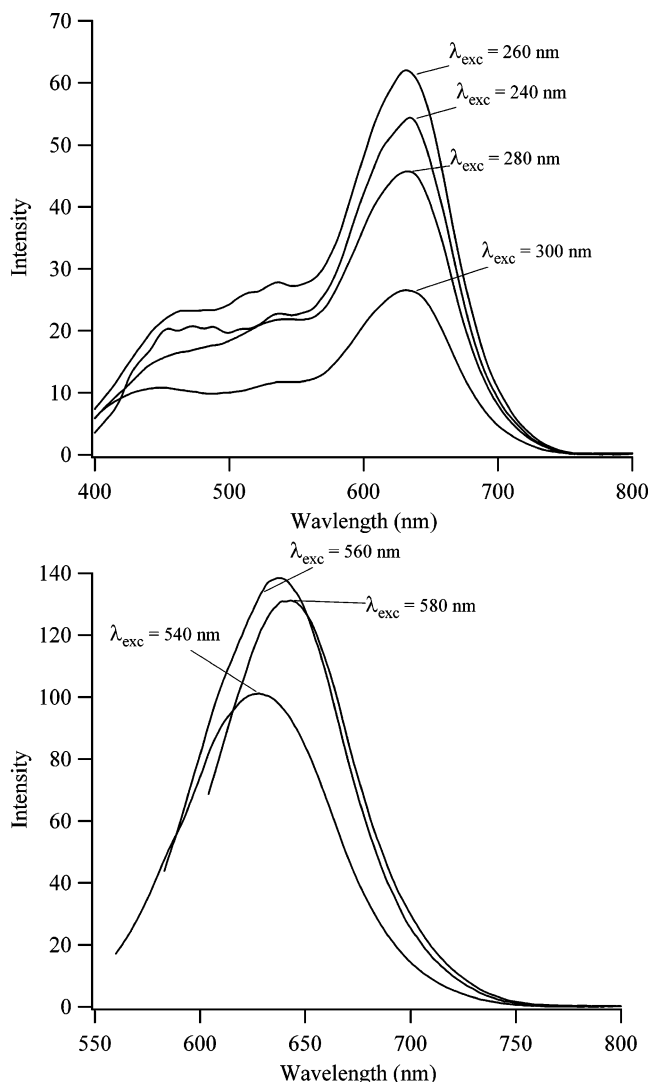


**Figure 6.** Fluorescence emission spectra of the silver nanoclusters bound to the oligonucleotide. For these spectra, [oligonucleotide] = 10  $\mu\text{M}$ ,  $[\text{Ag}^+] = 60 \mu\text{M}$ , and  $[\text{BH}_4^-] = 60 \mu\text{M}$ . In the top figure, a series of emission spectra were acquired using 240, 260, 280, and 300 nm excitation. A broad emission band is observed between 400 and 550 nm, and a peak is observed at 632 nm. In the bottom figure, excitation at 540, 560, and 580 nm results in emission bands with maxima at 629, 638, and 642 nm, respectively.

wavelengths with time. However, unlike the absorption spectra, the magnitude of this response does not diminish with time. A shoulder at 500 nm suggests the species that contribute to the longer wavelength absorptions (Figure 4) are also bound to the DNA strand.

As opposed to larger metal nanoparticles, a distinctive feature of small nanoclusters is their strong fluorescence due to their lower density of electronic states. For the DNA-bound nanoclusters, prominent fluorescence is observed at  $\sim 630 \text{ nm}$  (Figure 6). For excitation between 240 and 300 nm, a band at 630 nm is observed with the maximum intensity observed using 260-nm excitation. While this result suggests the cluster emission may occur via energy transfer, the silver clusters also have higher lying excited states accessible in this spectral region. Thus, emission following direct excitation of the higher electronic bands of the silver clusters is also feasible.

The multiple peaks in the absorption and circular dichroism spectra suggest the presence of small clusters with varying

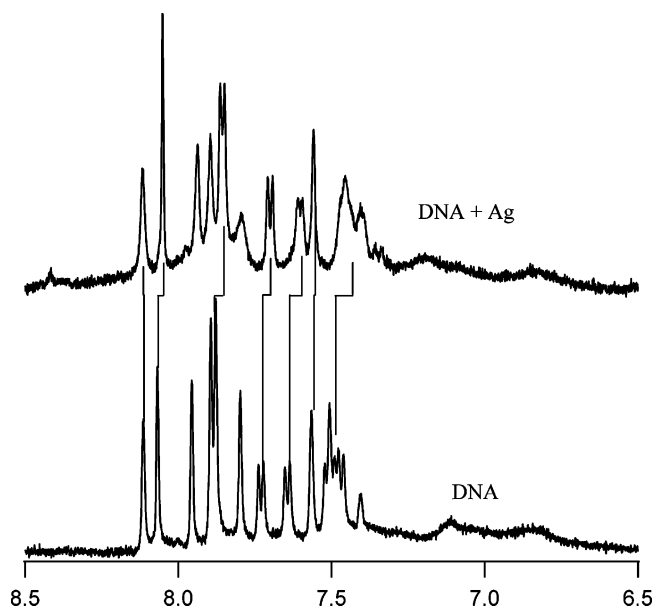


**Figure 7.** The aromatic proton region from  $^1\text{H}$  NMR spectra of the oligonucleotide with and without the silver nanoclusters. Vertical lines indicate aromatic proton resonances with chemical shifts that change after nanocluster formation. Cytosine H6 resonances, which exhibit the largest changes in chemical shift, can be identified by their splitting due to coupling to cytosine H5. For these spectra, [oligonucleotide] = 0.93 mM,  $[\text{Ag}^+] = 5.6$  mM, and  $[\text{BH}_4^-] = 5.6$  mM in a solution of 90% 1 mM phosphate buffer and 10%  $\text{D}_2\text{O}$  at 25  $^\circ\text{C}$ .

stoichiometries. The fluorescence spectra provide further evidence that the samples contain multiple species, but the mass spectra indicate that each DNA strand encapsulates only a single Ag nanocluster. First, the maximum emission intensity ( $\lambda_{\text{max}} = 638$  nm) occurs with an excitation wavelength of 560 nm (Figure 6), which is significantly red-shifted relative to the absorption maximum at 520 nm (Figure 4). Second, for excitation at wavelengths greater than 500 nm, the wavelength of maximum emission shifts to longer wavelengths as the excitation wavelength increases. One possibility suggested by Figure 6 is that the emission band for the 560-nm excitation can be spectrally decomposed as the emission bands for 540- and 580-nm excitation. In other words, at least two distinct species contribute to the fluorescence in this wavelength region.

As suggested by the absorption spectra, NMR spectra also indicate that the silver nanoclusters interact directly with the DNA bases. The aromatic proton resonances in the  $^1\text{H}$  NMR spectra of the oligonucleotide are well-resolved prior to the addition of  $\text{Ag}^+$  (Figure 7). However, the proton resonances are essentially broadened to baseline upon addition of  $\text{Ag}^+$  (spectrum not shown). In contrast, most of the aromatic proton resonances in the  $^1\text{H}$  spectra with silver clusters are almost as narrow as those of the free oligonucleotide (Figure 7). The cytosine H6 proton resonances exhibit the largest change in chemical shift in the presence of the silver nanoclusters (Figure 7). Similar upfield chemical shift changes were also observed for the H5 protons of cytosine (spectrum not shown). These observations indicate that the cytosine bases are most favored for interaction with the silver nanoclusters. The six cytosine H6 resonances were identified in 1D spectra based upon their splitting due to H6–H5 coupling and by H6–H5 cross-peaks in 2D COSY spectra. However, it was not possible to determine the sequence position of each cytosine resonance in the proton

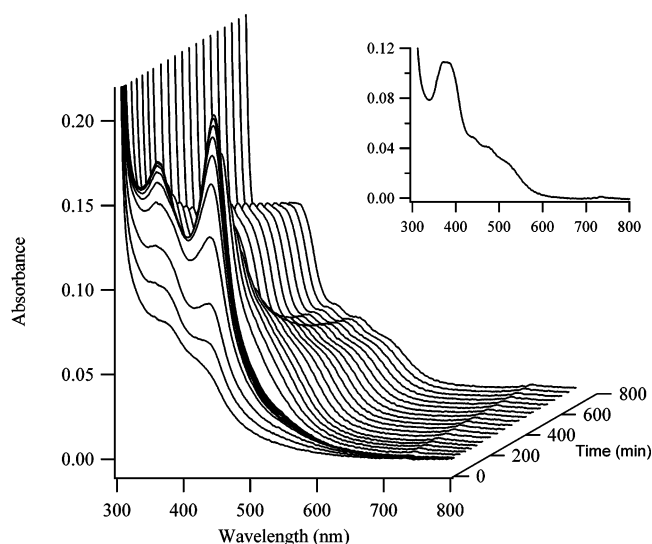


**Figure 8.** Absorption spectra associated with the DNA-bound silver nanoclusters using 1  $\text{Ag}^+$ :10 bases. For these spectra, [oligonucleotide] = 10  $\mu\text{M}$ ,  $[\text{Ag}^+] = 12$   $\mu\text{M}$ , and  $[\text{BH}_4^-] = 12$   $\mu\text{M}$ . The first 10 spectra were acquired every 2 min after adding the  $\text{BH}_4^-$ , and the spectrum at 20 min has  $\lambda_{\text{max}} = 440$  and 357 nm. Subsequent spectra were acquired approximately every 40 min. The inset spectrum shows the last spectrum in the series (704 min), and a peak at 380 nm is observed.

spectrum. Nevertheless, the different chemical shift changes exhibited by the cytosine H6 resonances indicate that cytosine bases interact with silver clusters in a sequence-dependent manner. Experiments with additional oligonucleotide sequences are necessary to properly assess the relative association of adenine, guanine, and thymine for silver nanoclusters.

**Concentration Studies.** To investigate the importance of the relative  $\text{Ag}^+$ :DNA stoichiometry, a 10  $\mu\text{M}$  concentration of the oligonucleotide was maintained while the  $\text{Ag}^+$  concentration was reduced from 1  $\text{Ag}^+$ :2 bases (Figure 4) to 1  $\text{Ag}^+$ :10 bases (Figure 8) and the cell path length was increased 5-fold. While the two sets of spectra are similar with respect to the overall absorbances and the wavelengths of the transitions, differences were observed. The maximum absorbance for the 420-nm peak occurred at 20 min for the more dilute sample, or about twice as long as for the more concentrated sample (Figure 4). This slower rate is expected when intermolecular exchange results in the formation of specific and favored cluster stoichiometries. The width of the 440-nm band is much narrower in the more dilute sample as opposed to the more concentrated sample, which suggests that a range of binding sites with slightly different electronic effects are available for binding by the silver clusters. At the lower concentration, the more favored sites are occupied, leading to an overall narrowing of the spectral transition. Another difference is the presence of a new band at 360 nm, and we observed no fluorescence associated with this band. Otherwise, no differences were observed in the fluorescence spectra of the concentrated and dilute samples.

## Conclusions

Small (<10 atoms) metallic nanoclusters have interesting optical properties and many potential applications, and we are interested in controlling their stoichiometry and, thus, their optical and electronic properties. Toward this goal, we have utilized DNA templates for synthesizing silver nanoclusters. From this work, we reach the major conclusions that DNA acts

as a template for the time-dependent and size-specific formation of nanoclusters. Prior to reduction, the  $\text{Ag}^+$  ions have a strong interaction with the DNA strands. Then, addition of  $\text{NaBH}_4$  results in 1–4 Ag atoms bound to the 12-base oligonucleotide, as determined through mass spectral analysis. The new electronic transitions that are observed in the absorption and fluorescence spectra are in the expected range for small silver nanoclusters. Base-specific interactions could be a significant feature of these nanoclusters, as suggested from the chemical shifts in the NMR spectra for the cytosine bases and the truncated distribution in the mass spectra. Together, these results suggest that it may be feasible to control the formation of nanoclusters with specific stoichiometries using DNA strands with specific sequences.

**Acknowledgment.** We appreciate the discussions with and the support of the following people: V. Conticello, Y. Zimenkov, Q. Darugar, S. Jain, S. Kanvah, U. Santhosh, and G. B. Schuster. J.P. gratefully acknowledges the support provided by the Research Site for Undergraduate Educators. R.M.D. thanks Olympus America Inc. for equipment loan and funding from the National Institutes of Health (1R01GM068731), the National Science Foundation (BES-0323453), the Vassar Wooley, Dreyfus, and Sloan Foundations, the Blanchard Endowment for Junior Faculty, and the Center for Advanced Research in Optical Microscopy at Georgia Institute of Technology.

JA031931O